



Variation patterns of extreme precipitation and relation to ocean-atmospheric climate in Sichuan province China from 1961 to 2017

Jun Li¹ · Yuandi Zhao¹ · Javed Iqbal²

Received: 8 August 2018 / Accepted: 20 January 2019 / Published online: 2 February 2019
© Springer-Verlag GmbH Austria, part of Springer Nature 2019

Abstract

Based on daily precipitation records in the Sichuan province, spatiotemporal changes in extreme precipitation from 1961 to 2017 and the relation to ocean-atmospheric climate were investigated. The trends and their statistical significance were computed with the nonparametric Sen's and Mann–Kendall tests. The characteristics of mutation and period were investigated with heuristic segmentation and continuous wavelet transform. The relations between extreme precipitation and ocean-atmospheric climate were diagnosed by cross-wavelet analysis. The results comprised three aspects. (1) The intensity, frequency, and duration of extreme precipitation increased in the Sichuan plateau, while the intensity and frequency of extreme precipitation decreased, but the duration of extreme precipitation did not change in the Sichuan basin. The contrary trends of extreme precipitation indices may have been influenced by the complex local geography, dramatically increased human activity, and source transportation of water vapor. (2) Temporally, the trends in extreme precipitation indices constituted slight changes in the Sichuan province. The Sichuan province experienced notable climate change because abrupt change points were observed for most of the extreme precipitation indices. Extreme precipitation was a fluctuation process from 1961 to 2017. (3) Because there was a decrease in precipitation during the warm phase periods of El Niño events and an increase during the cool phase periods of La Niña events in the Sichuan province, we show that the El Niño–Southern Oscillation (ENSO) has longer and stronger relations with extreme precipitation than the South Asian Summer Monsoon (SASM) or East Asian Summer Monsoon (EASM). The results of the present study will facilitate better decisions concerning preparedness for extreme precipitation events and management of water hazards in the Sichuan province.

1 Introduction

Extreme precipitations refer to an anomalous precipitation variable, which is lower than (or higher than) a threshold near the interval lower limit (or interval upper limit) of the variable precipitation observations (Alexander et al. 2006; Ma et al. 2013; Zhang et al. 2014b; Bi et al. 2017; Gao et al. 2018). An extreme precipitation event is an event that greatly impacts human society, such as a flash flood, drought, glacial lake

outburst flood (GLOF), debris flow, rock falls, or landslides. In recent years, many extreme precipitation events have occurred in China and have caused serious loss of human life and property. For example, a heavy rainstorm occurred in Tongren in the Guizhou province with a maximum 24-h rainfall of approximately 293.8 mm, which caused a loss of 0.14 billion RMB (Kong et al. 2017). A flash flood also killed hundreds of people in northern China on July 18–20, 2016. In addition, a rapid landslide affected the village of Xinmo in Maoxian County on June 24, 2017, which resulted in ten deaths and 73 missing persons under circulation of extreme precipitation (Fan et al. 2017; Yin et al. 2017). Therefore, many researches have focused on the investigation of increasing extreme precipitation events (She et al. 2013; Deng et al. 2018; Gao et al. 2018; Zhang et al. 2018; Zhao et al. 2018; Huang et al. 2018). To understand the changes in extreme precipitation, many researchers have examined the characteristics of extreme precipitation indices, and extreme precipitation exhibits apparent regional characteristics in China (Xu

✉ Jun Li
lijunxiaoyouxiang@163.com

¹ School of Civil Engineering, Sichuan University of Science and Engineering, Zigong 643000, China

² Department of Earth Sciences, COMSATS Institute of Information Technology, Abbottabad 22060, Pakistan

et al. 2011; Bi et al. 2017; Sun and Zhang 2017; Shi et al. 2018a), which are similar to those of worldwide extreme precipitation (Kenawy et al. 2011; Bezerra et al. 2018; Li et al. 2018; Iwona et al. 2018; Sedlmeier et al. 2018). Spatiotemporal variations of extreme precipitation indices have also been studied in different regions of China (Wang et al. 2013; Zhang et al. 2014a; Sun et al. 2016; Sigdel and Ma 2017). Total precipitation exhibits a good relationship with most extreme precipitation indices, and less than 10% of regional indices of extreme precipitation have significantly positive or negative trends in regions of China (Li et al. 2012a; Zhang et al. 2014b, 2015; Shi et al. 2018a).

The Sichuan province is a suitable region to comparatively analyze variations in extreme precipitation indices between higher altitudes and lower altitudes because of its unique terrain (Fig. 1). Several authors have investigated spatiotemporal variations of extreme precipitation in the Sichuan province (Hu et al. 2009; Bai et al. 2011). Annual precipitation significantly decreased in the western Sichuan basin but changed slightly in the eastern Sichuan basin (Bai et al. 2011). Hu et al. (2009) notes increasing trends were observed in the northwest Sichuan plateau and southwest Sichuan plateau, whereas decreasing trends were observed in the Sichuan basin. The

extreme precipitation of the southwest Sichuan plateau has a significantly increasing trend and a particularly dramatic increase occurred in the beginning of the 1980s. The trends of the Sichuan basin and the northwest Sichuan plateau are decreasing, but not significantly (Zhang and Ma 2011). Normal drought was observed in the western Sichuan basin, whereas normal increasing drought was observed in the southern Sichuan basin. Precipitation changed abnormally in the central basin, which exhibited both increased drought and precipitation intensity, irrespective of the total precipitation (Zhou and Lei 2018). However, multiple indices of extreme precipitation were not utilized in previous studies. Moreover, some key indices have not been discussed in the context of the Sichuan province. Differences in the climatic variability of the Sichuan province have not been fully explored, and the sensitivity of the Sichuan province to climate change cannot be accurately determined without such work. Therefore, in the present study, changes in extreme precipitation are determined using multiple indices of extreme precipitation and the relation to ocean-atmospheric climates is analyzed. The results of this study will guide decisions concerning the management of regional water resources and the prevention of water hazards.

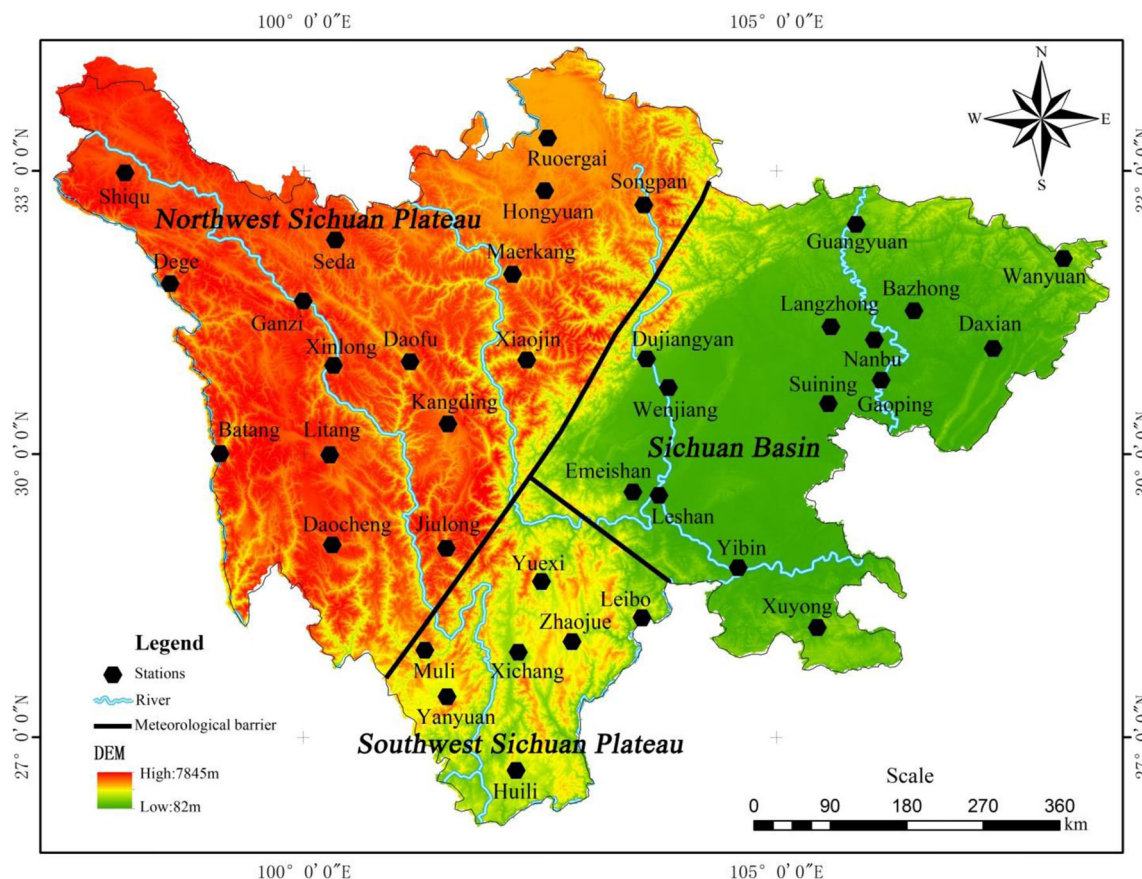


Fig. 1 Sichuan province

2 Study area, data, and methodology

2.1 Study area

The Sichuan province is located between the Tibet plateau and the Central China plain. The area of Sichuan province is 56.76×10^4 km² and its local terrains are unique. The east of the Sichuan province is a basin named the Sichuan basin (elevation from 300 to 700 m), which belongs to the second step of China's terrain. The west of the Sichuan province is characterized by mountain plateaus containing the northwest Sichuan plateau (elevation of ridges from 4000 to 5000 m) and the southwest Sichuan plateau (elevation of ridges from 3500 to 4000 m), both in the first step of China's terrain. The boundaries around the northwest Sichuan plateau, southwest Sichuan plateau, and Sichuan basin are the Longmenshan and Daliangshan mountains (Fig. 1).

2.2 Data

Daily precipitation data from 1961 to 2017 from 37 meteorological stations were selected to observe the changes in extreme precipitation in the Sichuan province and its subregions, i.e., the northwest Sichuan plateau, southwest Sichuan plateau, and Sichuan basin. The basic information and spatial distribution of the selected stations are shown in Fig. 1 and Table 1, respectively. The daily precipitation data were downloaded from the China Meteorological Administration (CMA) for 1961–2017.

The data quality control procedures are comprised of two parts. First, from March 2011 to June 2012, basic quality control for all national meteorological stations were completed by the CMA. The missing data of each station are shown in Table 1. Fifty-four percent of stations have a complete series of daily precipitation data. Thirty-two percent of stations have missing data between 1 and 30 days only which is acceptable for analysis and interpretation. The missing data of 15% stations are more than a month, and Litang is the only station which shows the missing data of 384 days. Stations with missing data series were interpolated with daily grid precipitation data of $0.5^\circ \times 0.5^\circ$ in China, and the interpolation series passed the homogenization test by the RHtest V4. RClimdex V1 software was used to identify erroneous precipitation data and potential outliers during the first run, e.g., precipitation values below 0 mm. In this study, those outliers were manually validated, removed, or corrected. Then, combining the station metadata of the Sichuan province and the Penalized Maximal F test (PMF), RHtest V4 software was utilized to observe the multiple change points in the daily precipitation data series of all stations. The results reveal that not all stations have change points, except

for Xuyong, Yanyuan, and Shiqu stations. The change points occurred in April 2015, August 2002, and September 2016, respectively, at the three stations. After checking the metadata of these stations, no relocations or undated instruments occurred in that period, and the three stations do not have true change points. Therefore, all stations passed the homogeneity tests. The principles of RClimdex V1 software and RHtest V4 software have been discussed in detail in one study by Wang (2008a, b).

The World Meteorological Organization recommends the 11 extreme precipitation indices shown in Table 2 (Karl et al. 1999). The indices of extreme precipitation are divided into two categories, precipitation day indices and precipitation indices. The duration of extreme precipitation is represented by CDD, CWD, R10, R20, and R25. The intensity of extreme precipitation is represented by RX1day, RX5day, and SDII. The frequency of extreme precipitation is represented by R95, R99, and PRCPTOT.

2.3 Methodology

The trends of extreme precipitation indices were investigated in Sichuan province, whereas trend differences were compared among the northwest Sichuan plateau, the southwest Sichuan plateau, and the Sichuan basin. In addition, the mutation characteristic and periodic characteristic were delineated. We also elucidated the relation between the ocean-atmospheric climate indices and the extreme precipitation indices. The methods for analyzing indices are comprised of four parts. First, the indices of extreme precipitation were calculated by RClimDex software. Second, the indices trends were computed by MAKESENS software using the nonparametric Sen's method (Salmi et al. 2002). The statistically significant of trends at the 5% level was checked by the Mann–Kendall test. Origin 2015 and ArcGIS 10.1 software were used to illustrate the temporal and spatial variations of indices trends, respectively. Third, cross-wavelet analysis and the Mann–Kendall test were employed to determine the periodic and mutation characteristics of extreme precipitation. Fourth, relations between the indices of ocean-atmospheric climate and the extreme precipitation indices were investigated by cross-wavelet analysis and Pearson's correlation.

2.3.1 Sen's method

If a trend can be assumed to be linear, Sen's method can be utilized to compute the trend slope (Gilbert 1988). The equation of Sen's method is shown in Eq. (1):

$$f(t) = Qt + B \quad (1)$$

Table 1 Stations in Sichuan province

Region	Station name	WMO number	East longitude	North longitude	Elevation (m)	Missing data
Sichuan basin	Wenjiang	56,187	103.52	30.45	547.7	None
	Dujiangyan	56,188	103.4	31	698.5	None
	Emeishan	56,385	103.2	29.31	3047.4	None
	Leshan	56,386	103.45	29.34	424.2	None
	Yibin	56,492	104.36	28.48	340.8	2 days
	Guangyuan	57,206	105.51	32.26	513.8	66 days
	Wanyuan	57,237	108.02	32.04	674	1 day
	Langzhong	57,306	105.58	31.35	382.6	None
	Bazhong	57,313	106.46	31.52	417.7	1 day
	Nanbu	57,314	106.04	31.21	405.7	None
	Daxian	57,328	107.3	31.12	344.9	124 days
	Suining	57,405	105.33	30.3	355	1 day
	Gaoping	57,411	106.06	30.47	309.7	None
	Xuyong	57,608	105.26	28.1	377.5	None
	Northwest Sichuan plateau	Shiqu	56,038	98.06	32.59	4200
Ruoergai		56,079	102.58	33.35	3441.4	1 day
Dege		56,144	98.35	31.48	3184	1 day
Ganzi		56,146	100	31.37	3393.5	None
Seda		56,152	100.2	32.17	3893.9	2 day
Daofu		56,167	101.07	30.59	2957.2	None
Maerkang		56,172	102.14	31.54	2664.4	1 day
Hongyuan		56,173	102.33	32.48	3491.6	None
Xiaojin		56,178	102.21	31	2438	None
Songpan		56,182	103.36	32.4	2850.7	None
Batang		56,247	99.06	30	2589.2	245 days
Xinlong		56,251	100.19	30.56	3000	None
Litang		56,257	100.16	30	3948.9	384 days
Daocheng		56,357	100.18	29.03	3727.7	31 days
Kangding		56,374	101.58	30.03	2615.7	8 days
Southwest Sichuan plateau	Jiulong	56,462	101.3	29	2925	None
	Muli	56,459	101.16	27.56	2426.5	None
	Yuexi	56,475	102.31	28.39	1659.5	None
	Zhaojue	56,479	102.51	28	2132.4	None
	Leibo	56,485	103.35	28.16	1255.8	None
	Yanyuan	56,565	101.31	27.26	2545	2 days
	Xichang	56,571	102.16	27.54	1590.9	1 day
Huili	56,671	102.15	26.39	1787.3	None	

Where Q is the slope of extreme precipitation indices, B is the constant of extreme precipitation indices, $f(t)$ is the continuously monotonic function of time, and t is the daily precipitation data series from 1961 to 2017.

2.3.2 Mann–Kendall test

For the Mann–Kendall test, it is not essential that the data series obey distributions, and this test is not constrained by a few abnormal anomalies (Jaagus 2006). Therefore, we utilized

this method to compute the significance of trends in extreme precipitation indices.

2.3.3 Heuristic segmentation method

This method was introduced to determine the mutation characteristics of extreme precipitation (Bernaolagalván et al. 2001; Liu and Xu 2016). The difference in statistical significance $T(i)$ was calculated by Eq. (2). The largest difference in statistical significance T can be obtained in a data series, which

Table 2 Descriptions of extreme precipitation indices recommended by the World Meteorological Organization

Category	Indices	Unit	Full name
Precipitation days indices	CDD	d	Consecutive dry days
	CWD		Consecutive wet days
	R10		Heavy precipitation days
	R20		Very heavy precipitation days
	R25		Extremely heavy precipitation days
Precipitation indices	RX1day	mm	Highest precipitation amount of maximum 1 day
	RX5day		Highest precipitation amount of maximum 5 days
	R95		Precipitation on very wet days
	R99		Precipitation on extremely wet days
	PRCPTOT		Annual total wet day precipitation
	SDII	mm/d	Simple daily intensity index

can represent the change point. We used Eq. (3) to compute the statistical significance $P(t_{max})$ corresponding to T . If the statistical significance is lower than the threshold of 0.95, then the signal will not be divided into two parts; otherwise, the series should be divided into two subsequences at that point. The iteration procedure continues recursively for each of the two subsequences until $P(t_{max}) < 0.95$ or the segment length l_0 is less than 30.

$$T(i) = \left| \frac{\bar{x}_1 - \bar{x}_2}{s(i)} \right| \tag{2}$$

$$s(i) = \sqrt{\frac{(n_1 - 1) \times s_1 + (n_2 - 1) \times s_2}{n_1 + n_2 - 2}} \times \left(\frac{1}{n_1} + \frac{1}{n_2} \right) \tag{3}$$

$$P(t_{max}) \approx \left[1 - I_{\left[\frac{\nu}{\nu + T^2_{max}} \right]}(\delta\nu, \delta) \right]^\eta \tag{4}$$

where $T(i)$ is the difference in statistical significance, \bar{x}_1 and \bar{x}_2 represent the left and right mean values, respectively, s_1 and s_2 represent the left and right standard deviations, respectively, $s(i)$ is the pooled variance, n_1 and n_2 are the length of the two side parts in a time series, $P(t_{max})$ is the statistical significance, $I_{\left[\frac{\nu}{\nu + T^2_{max}} \right]}(\delta\nu, \delta)$ is the incomplete beta function, η is equal to $4.19 \times \ln(N) - 11.54$ based on the simulation of Monte Carlo, ν is equal to $n - 2$, and δ is equal to 0.4.

2.3.4 Cross-wavelet analysis

Compared with Fourier transform, the cross-wavelet analysis is more suitable to delineate the cross spectrum and oscillations of two-time series (Huang et al. 2015). Cross-wavelet analysis contains the continuous-wavelet transform (CWT) and the cross-wavelet transform (XWT) (Jevrejeva et al. 2003; Grinsted et al. 2004). The relations between indices of extreme precipitation and the ocean-atmospheric climate indices were analyzed using the XWT. In addition, the periodic characteristics of extreme precipitation were calculated by the XWT embedded in the CWT program.

The ocean-atmospheric climate indices contain the South Asian Summer Monsoon Index (SASMI), the East Asian Summer Monsoon Index (EASMI) and the Multivariate ENSO Index (MEI). The EASMI and SASMI were obtained from the Li Jianping research group, and the MEI was obtained from the National Oceanic and Atmospheric Administration of the USA (Wolter and Timlin 2011).

3 Results

3.1 Spatial change characteristics of extreme precipitation indices

The duration of extreme precipitation indices increased in the Sichuan plateau, whereas the indices' duration remained stationary in the Sichuan basin. Moreover, the intensity and frequency of extreme precipitation indices decreased in the Sichuan basin and increased in the Sichuan plateau.

3.1.1 Precipitation days indices

The trends were slightly decreasing in the middle of the Sichuan basin, whereas slightly increasing trends and stationary trends are observed in the southwest Sichuan plateau and northwest Sichuan plateau, respectively. This demonstrates that the duration of extreme precipitation indices will possibly decrease in the middle of the Sichuan basin. The 48.6% of precipitation day indices exhibited stationary trends, including CWD, R20, and R25. This suggests that the duration of extreme precipitation will not change. Moreover, the ratio of statistically significant trends in the precipitation day indices was 6%, which indicates that the changes in precipitation day indices were obvious in the Sichuan province (Fig 2).

The CDD had slightly increasing trends which cover a large part of the Sichuan province. Ten stations located in the outermost area of the northwest Sichuan plateau exhibited

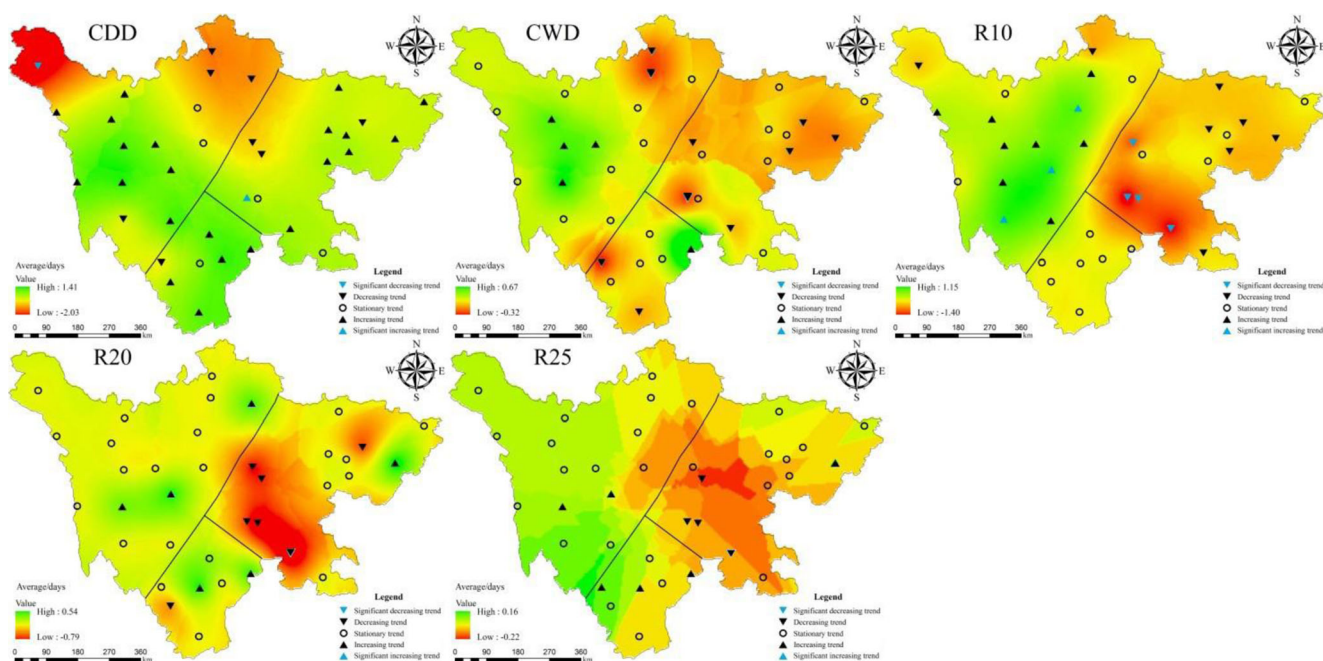


Fig. 2 Trend changes in precipitation day indices in the Sichuan province from 1961 to 2017. The color indices distributions were computed and drawn with ArcGIS 10.1 using the Kriging interpolation method

slightly decreasing trends. Four stations located in the middle of Sichuan province had stationary trends. The increasing trends ranged from 0.3 to 3.33 d/10a and the decreasing trends ranged from -0.22 to -4.29 d/10a. Two stations, Emeishan station and Shiqu station, exhibited statistically significant trends of 1.21 and -4.29 d/10a, respectively. These results show that the occurrence of drought will increase in this region.

For CWD, the spatial distributions of trends were irregular. Twenty-two stations had stationary trends in the Sichuan province, five stations had slightly increasing trends from 0.27 to 1.37 d/10a, and ten stations exhibited slightly decreasing trends from -0.2 to -0.69 d/10a in the Sichuan plateau. Decreasing trends were observed in 16% of stations, from 0.24 to 0.69 d/10a. These results suggest that consecutive wet days will not change in a large part of the Sichuan province.

For R10, R20, and R25, the western Sichuan basin exhibited slightly decreasing trends, and the trends in R10 were mostly statistically significant. Consequently, the duration of R10, R20, and R25 will decrease in this region.

For R10, the trends in the southwest Sichuan plateau are stationary. Large parts of the northwest Sichuan plateau showed slightly increasing trends. Three stations showed increasing trends from 0.95 to 1.14 d/10a. Moreover, large parts of the Sichuan basin exhibited negative slopes. Four stations showed decreasing trends from -0.91 to -1.43 d/10a.

For R20 and R25, 67% of stations are stationary in large parts of the Sichuan province, except for the middle of the Sichuan basin. In case of R20, seven stations exhibited

slightly decreasing trends. Seven stations showed slightly increasing trends. For R25, six stations exhibit slightly increasing trends. Four stations showed slightly decreasing trends, including Yibin station with a trend of -0.64 d/10a.

3.1.2 Precipitation indices

Considering the precipitation indices, the Sichuan basin exhibits slightly decreasing trends, as shown in Fig. 3. The northwest Sichuan plateau showed obviously increasing trends, except for R99. The southwest Sichuan plateau exhibited both increasing trends and decreasing trends, except for R99. Statistically significant trends of indices were observed in 11% of stations.

The results of RX1day, RX5day, and SDII suggest that the intensity of extreme precipitation decreased in the middle Sichuan basin and a large part of the southwest plateau, whereas extreme precipitation increased in the west and northeast Sichuan province. The extreme precipitation indices (R95 and PRCPTOT) results reveal that the frequency of extreme precipitation decreased in the Sichuan basin, whereas the frequency of extreme precipitation increased in the Sichuan plateau.

For RX1day, the west and northeast Sichuan province (24 stations) exhibited increasing trends of 0.05–5.03 mm/10a and other regions of the Sichuan province (22 stations) showed decreasing trends, except for Wenjiang station. Four stations showed statistically significant trends. Yibin station showed a statistically significant trend of -5.94 mm/10a, and Muli, Kangding, and Litang stations showed statistically significant

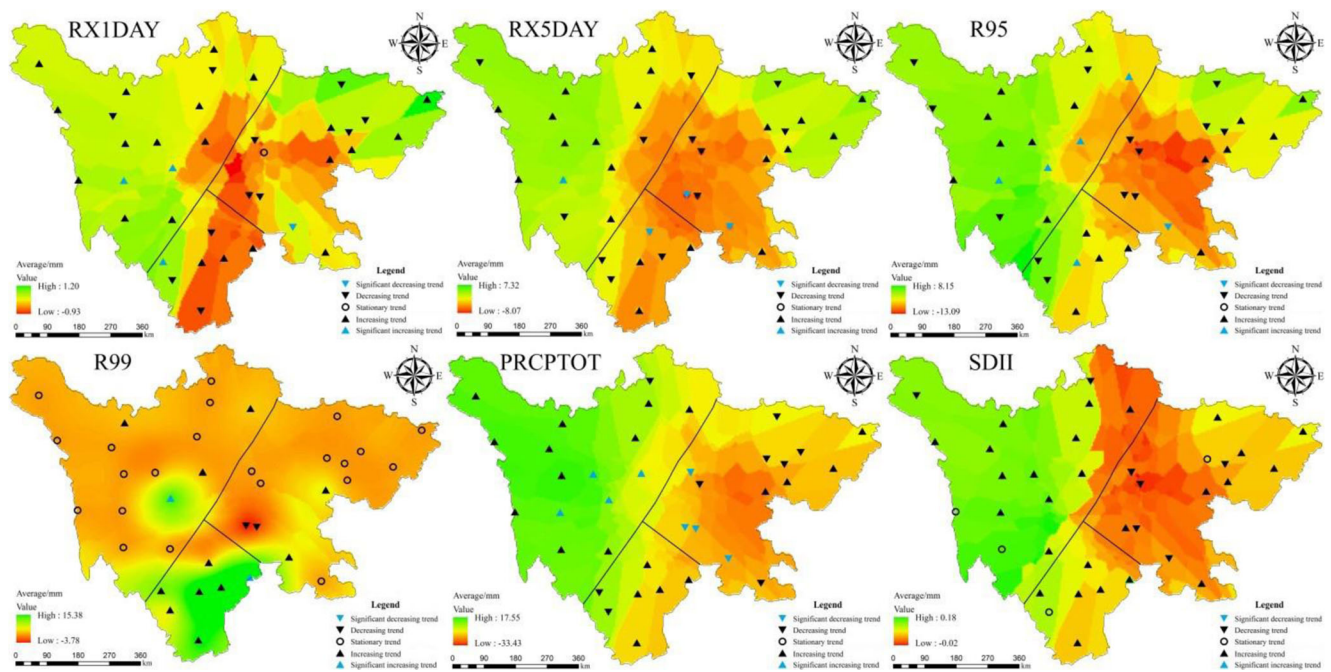


Fig. 3 Trends in extreme precipitation indices in the Sichuan province from 1961 to 2017. The color indices distributions were computed and illustrated with ArcGIS 10.1 using the Kriging interpolation method

trends of 1.84 mm/10a, 1.1 mm/10a, and 1.83 mm/10a, respectively.

The spatial distributions of RX5day are similar to those of the RX1day. Western and northeastern Sichuan province (22 stations) exhibited increasing trends of 0.04–11.31 mm/10a, whereas the middle Sichuan basin and a large part of the southwest plateau (15 stations) show decreasing trends of -0.12 – 10.77 mm/10a. Five stations showed statistically significant trends, from -10.77 to 4.47 mm/10a. Litang station exhibited the maximum significantly increasing trend and Emeishan station exhibited the minimum significantly decreasing trend.

For R95, the western and northeastern Sichuan province (23 stations) exhibited increasing trends of 0.16–30.34 mm/10a, whereas the middle Sichuan basin and a large part of the southwest plateau (14 stations) showed decreasing trends of 0.25–37.71 mm/10a. The maximum increasing trend of 30.34 mm/10a was observed in Xichang station and this trend is statistically significant. The maximum decreasing trend of 37.71 mm/10a was observed in Yibin station and this trend is statistically significant.

For R99, the southwest Sichuan plateau showed obviously increasing trends of 1.27–15.5 mm/10a and the trends of other regions are mostly stationary. Stationary trends were observed in 22 stations and increasing trends were observed in 13 stations. Decreasing trends of -3.87 mm/10a and -2.76 mm/10a were observed at Emeishan and Leshan stations, respectively.

For PRCPTOT, the eastern Sichuan province exhibited an obviously decreasing trend of 9.02–60.31 mm/10a and the

western Sichuan province exhibited an obviously increasing trend of 0.61–31.12 mm/10a. Twenty-four stations showed increasing trends and the other stations have decreasing trends. The northwest Sichuan plateau showed a significantly increasing trend, and Kangding station showed the maximum significantly increasing trend of 31.12 mm/10a. Moreover, Dafu, Xiaojin, and Litang stations showed significantly increasing trends of 15.94 mm/10a, 12.63 mm/10a, and 28.95 mm/10a, respectively. Dujiangyan, Emeishan, Leshan, and Yibin stations along the Minjiang river in the Sichuan basin showed significantly decreasing trends, with values greater than 30 mm/10a.

For SDII, the trends of all stations are not statistically significant. Most stations have slight increasing trends.

3.2 Regional trends in extreme precipitation indices

Temporally, the trends constitute slight changes in the Sichuan province. The Sichuan basin exhibited mostly decreasing trends, whereas the northwest and southwest Sichuan plateaus showed slightly increasing trends. Concerning seasonal changes in extreme precipitation, spring, summer, and winter showed increasing trends, whereas autumn exhibited a decreasing trend. Sichuan province and three subregions experience notable climate change because abrupt change points were observed in many indices of extreme precipitation. Most indices have a characteristic 4–8-year period and passed the 95% confidence level. RX1day has long periods with a 6-year oscillation signal and a 12-year oscillation signal, and R95 has a long period with a 4–8-year signal.

3.2.1 Precipitation days indices

For the indices of precipitation days, the regional trends of five indices are small, and even R10, R20, and R25 exhibit stationary slopes. This demonstrates that the indices of precipitation days did not change from 1961 to 2017 (Fig. 4) (Table 3).

The CDD showed a slightly increasing trend of 0.47 d/10a. The CDD in 2013 exhibited the maximum anomaly of 78.08 days and the CDD in 1961 showed the minimum anomaly of 32.28 days. The average regional anomaly was 52.32 days in the Sichuan province. The CDD is an indicator of the dry season length, according to the predominance of the regional monsoonal climate.

The CWD exhibited a slightly decreasing trend of -0.02 d/10a in the precipitation day indices. The average regionally anomaly was 9.29 days from 1961 to 2017. The maximum anomaly of 11.3 days was observed in 2011 and has the minimum anomaly of 7.62 days was observed in 1964.

The trends of R10 and R25 were 0.01 d/10a, and the R20 showed a stationary trend. The maximum anomalies of R10, R20, and R25 were observed in 1998. The maximum anomalies of R10, R20, and R25 were 30.32 days, 11.92 days, and 8.84 days, respectively. The R10 showed the minimum anomaly of 21.65 days in 1969. The R20 and R25 showed the minimum anomalies of 7.38 and 4.92 days in 1972 and 1997, respectively.

3.2.2 Precipitation indices

R95 and R99 showed clearly increasing trends of 2.2 and 2.91 mm/10a, respectively. Other indices of precipitation exhibited slightly positive slopes, which were less than 1 mm/10a. Most precipitation indices were not statistically significant (Fig. 5; Table 4).

RX1day showed a regional trend of 0.26 mm/10a. The average anomaly was 65.6 mm from 1961 to 2017. The RX1day showed the maximum anomaly of 88.29 mm in 2013 and the minimum anomaly of 48.91 mm in 1976.

The regionally increasing trend of RX5day was 0.51 mm/10a. The average anomaly was 114.95 mm. The RX5day of 2013 showed a maximum anomaly of 149.25 mm and a minimum anomaly of 93.84 mm in 2006. The regional trends of RX1day and RX5day are similar.

R95 and R99 showed similarly increasing trends of 2.2 and 2.91 mm/10a, respectively. The average anomalies of R95 and R99 were 288.35 and 95.85 mm, respectively. For R95, 1998 exhibited the maximum anomaly of 380.68 mm, and 1972 had the minimum anomaly of 210.29 mm. For R99, 2013 showed the maximum anomaly of 140.19 mm, and 1976 showed the minimum anomaly of 33.9 mm.

SDII exhibited a slightly increasing trend of 0.11 mm/10a. The SDII showed a maximum anomaly of 10.46 mm in 2013 and a minimum anomaly of 8.93 mm in 1977. The average anomaly was 10.46 mm/10a.

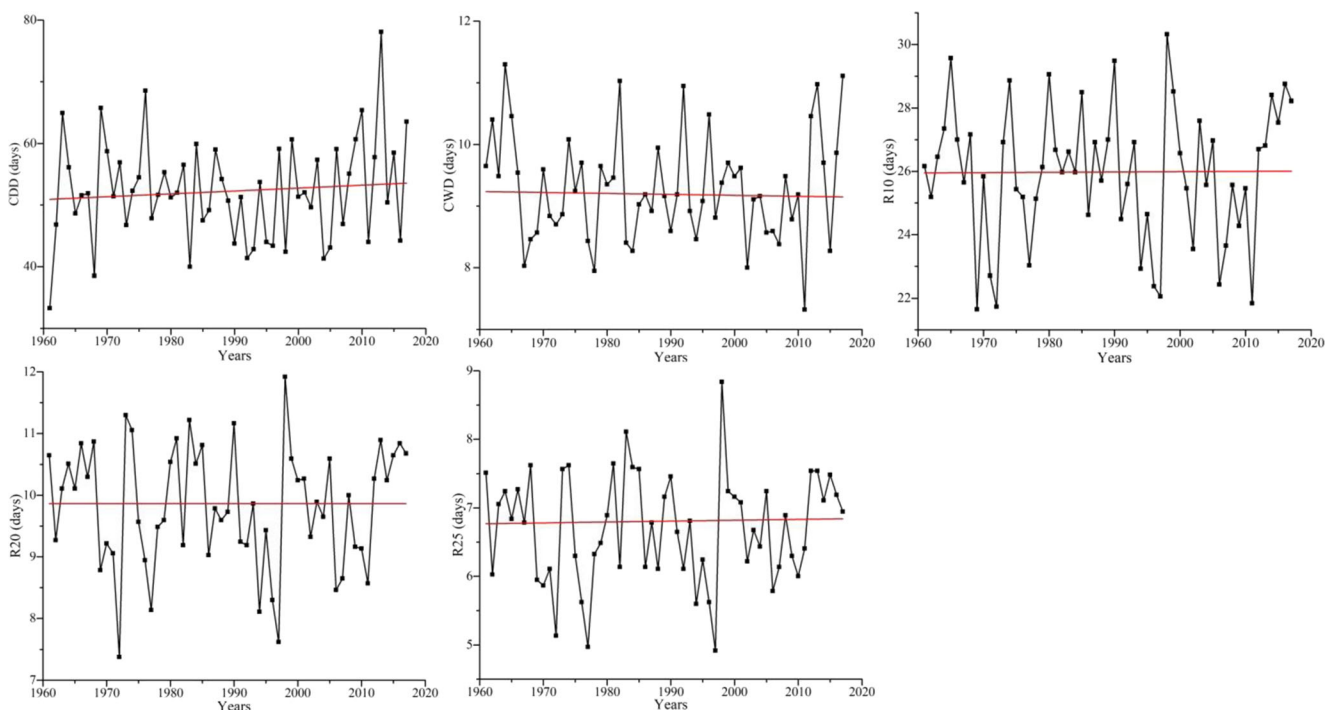


Fig. 4 Temporal changes in trends for precipitation day indices (CDD, CWD R10, R20, and R25). The black line is an indices data series from 1961 to 2017. The red line is the linear trend slope of extreme precipitation indices

Table 3 Decadal trend rates (d/10a) of precipitation day indices in the Sichuan province

Index	Trend	Average anomalies	Max. anomalies	Max. year	Min. anomalies	Min. year
CDD	0.47	52.32	78.08	2013	32.28	1961
CWD	-0.02	9.29	11.3	2011	7.62	1964
R10	0.01	25.91	30.32	1998	21.65	1969
R20	0.00	9.81	11.92	1998	7.38	1972
R25	0.01	6.70	8.84	1998	4.92	1997

PRCPTOT exhibited a positive slope of 0.18 mm/10a. The average anomaly was 882.45 mm/10a. For PRCPTOT, 1998 had the maximum anomaly of 1018.01 mm and 2006 had the minimum anomaly of 749.85 mm.

3.2.3 Regional trend differences in extreme precipitation indices

In order to highlight the spatial differences and regional characteristics, we divided the Sichuan province into three subregions according to the specification of China’s meteorological and geographical regionalization (Table 5). For the 11 extreme precipitation indices, the average anomalies in the northwest Sichuan plateau are generally the smallest, except for CDD, CWD, and SDII. This indicates that the change magnitude of extreme precipitation is not obvious in the northwest Sichuan plateau. The changes in extreme precipitation indices are increasing, except for RX5day in the northwest and southwest Sichuan plateau. This demonstrates that the duration intensity and frequency of extreme precipitation increased

in the three subregions. In addition, increasing trends and decreasing trends were observed in the Sichuan basin. Statistically significant ratios of indices occurred in 12% of the three subregions.

For precipitation day indices, slightly decreasing trends from -0.11 to -0.44 d/10a were observed, except for CDD in the Sichuan basin. The northwest and southwest Sichuan plateau exhibited slightly increasing trends from 0.05 to 0.65 d/10a. CWD in the Sichuan basin exhibited a trend of -0.23 d/10a. For R20 and R25, the average anomalies from high to low belong to the Sichuan basin, the southwest Sichuan plateau, and the northwest Sichuan plateau. For CDD, the northwest Sichuan plateau showed the maximum average anomaly of 68.93 mm and the average anomalies of the Sichuan basin and the southwest Sichuan plateau are 28.61 and 61.77 mm, respectively. For CWD, the average anomalies of the three regions are similar and ranged from 6.86 mm to 12.79 mm. For R10, the average anomalies from high to low belong to the southwest Sichuan plateau, the Sichuan basin, and the northwest Sichuan plateau.

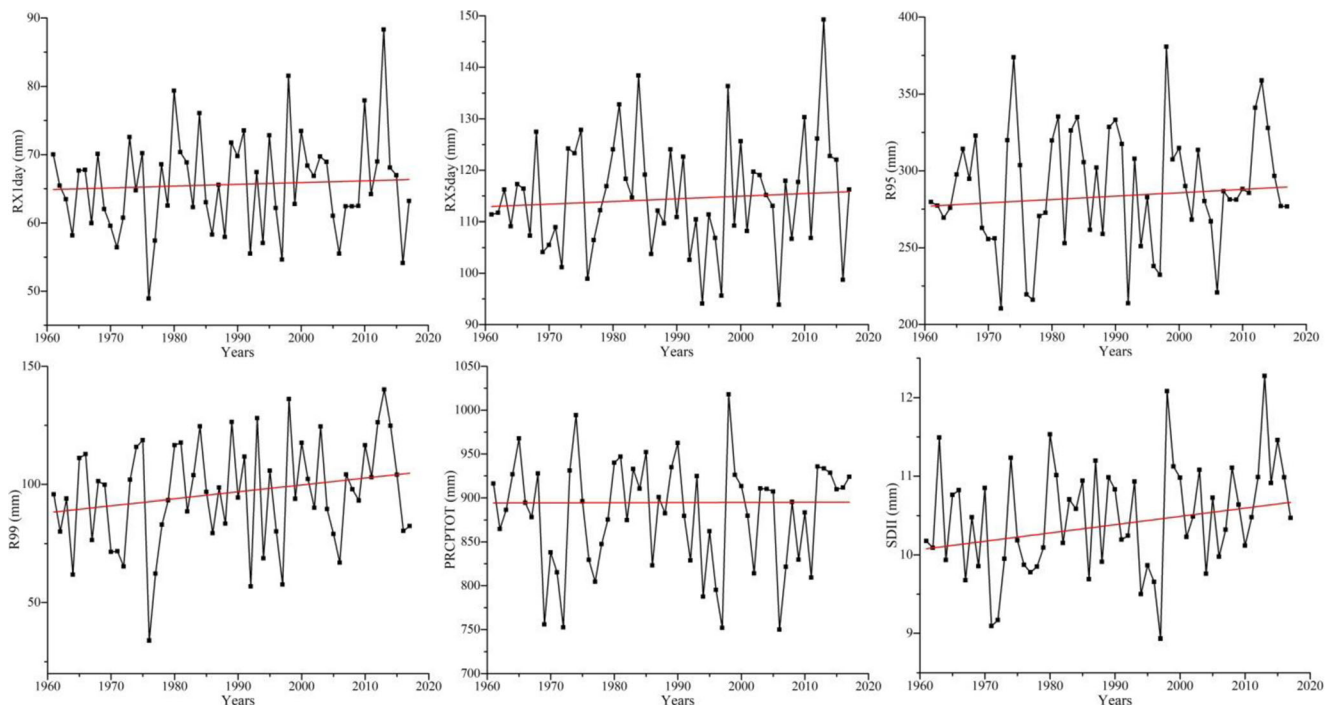


Fig. 5 Temporal changes in trends of precipitation indices (RX1day, RX5day, R95, R99, SDII, and PRCPTOT)

Table 4 Decadal trend rates (mm/10a) of extreme precipitation indices in the Sichuan province

Index	Trend	Average anomalies	Max. anomalies	Max. year	Min. anomalies	Min. year
RX1day	0.26	65.60	88.29	2013	48.91	1976
RX5day	0.51	114.95	149.25	2013	93.84	2006
R95	2.20	288.35	380.68	1998	210.29	1972
R99	2.91	95.82	140.19	2013	33.90	1976
SDII	0.11	10.46	12.28	2013	8.93	1997
PRCPTOT	0.18	882.45	1018.01	1998	749.85	2006

For the precipitation indices, PRCPTOT exhibited the largest trends of the three regions. The PRCPTOT of the northwest Sichuan plateau, the southwest Sichuan plateau, and the Sichuan basin exhibited slopes of 13.99 mm/10a, 7.73 mm/10a, and -15.47 mm/10a, respectively. The trend of the northwest Sichuan plateau is statistically significant. Three decreasing trends and three increasing trends were observed in the Sichuan basin; however, they are not statistically significant. In the northwest Sichuan plateau, the precipitation indices exhibited increasing trends from 0.16 to 13.99 mm/10a. Those of R95, R99, and PRCPTOT are statistically significant. In the southwest Sichuan plateau, increasing trends were observed in precipitation indices except for RX5day. R99 exhibited statistically significant trends of 9.72 mm/10a. For RX1day, RX5day, and PRCPTOT, the average anomalies from high to low were observed in the Sichuan basin, the southwest Sichuan plateau, and the northwest Sichuan plateau. For R95 and R99, the average anomalies from high to low are from the southwest Sichuan plateau, the Sichuan basin, and the northwest Sichuan plateau. The average anomalies of SDII of the three subregions vary only slightly (Table 5).

3.2.4 Seasonal change characteristics of extreme precipitation indices

We choose the RX1day and RX5day indices to observe the seasonal change characteristics of extreme precipitation. Increasing trends were observed in spring, summer, and winter, whereas decreasing trends are observed in autumn, as shown in Table 6. However, these trends are not statistically significant. From spring to winter, except for autumn, the trends first increase and then decrease. The maximum increasing trends of RX1day and RX5day were 1.33 and 2.3 mm/10a, respectively. The maximum decreasing trends of RX1day and RX5day were -0.94 and -2.49 mm/10a, respectively.

Table 7 presents the seasonal changes in indices in the three subregions. Concerning the northwest Sichuan plateau, increasing trends were observed in each season. Statistically significant trends of RX1day or RX5day were detected in spring. The maximum trends of RX1day and RX5day were 1.48 and 2.8 mm/10a, respectively. For the southwest Sichuan plateau, the spring and summer of RX1day and RX5day exhibited increasing trends from 0.28–3.67 mm/10a, whereas the autumn and winter showed decreasing trends from -0.14 to -0.73 mm/10a. RX5day exhibited a statistically

Table 5 Decadal trend rates of indices in three subregions

Category	Index	Sichuan basin		Northwest Sichuan plateau		Southwest Sichuan plateau	
		Average anomaly	Trend	Average anomaly	Trend	Average anomaly	Trend
Precipitation day indices	CDD	28.61	0.65	68.93	0.23	61.77	0.65
	CWD	6.86	-0.23	9.88	0.05	12.79	0.06
	R10	29.02	-0.44	21.03	0.53	30.84	0.19
	R20	14.43	-0.21	4.50	0.14	12.73	0.16
	R25	10.94	-0.11	2.20	0.08	8.51	0.25
Precipitation indices	RX1day	106.98	-0.32	31.15	0.49	61.60	0.81
	RX5day	169.64	0.58	69.06	1.05	110.45	-0.18
	R95	356.92	-2.38	126.30	<i>4.61</i>	521.59	10.63
	R99	120.78	0.34	36.35	<i>2.24</i>	181.82	<i>9.72</i>
	SDII	10.91	0.06	10.34	0.16	9.83	0.15
	PRCPTOT	1106.66	-15.47	658.29	<i>13.99</i>	946.38	7.73

Italic values indicate that the trends of indices are statistically significant at the 5% level

Table 6 Decadal trend rates (mm/10a) of indices in the Sichuan province

Index	Spring		Summer		Autumn		Winter	
	Average value	Trend	Average value	Trend	Average value	Trend	Average value	Trend
RX1day	51.44	1.01	135.33	1.33	66.47	-0.94	10.87	0.21
RX5day	86.10	1.21	241.29	2.30	126.46	-2.49	19.43	0.08

significant trend of 3.67 mm/10a in spring. For the Sichuan basin, increasing trends and decreasing trends were observed in each season; however, they are not statistically significant. The maximum increasing trends of RX1day and RX5day were 1.41 and 4.06 mm/10a, respectively, both in summer. The maximum decreasing trends of RX1day and RX5day were -1.79 and -3.93 mm/10a, both in autumn. In addition, the average values from high to low occurred in the Sichuan basin, the northwest Sichuan plateau, and the southwest Sichuan plateau.

3.3 Other temporal change characteristics in the extreme precipitation indices

3.3.1 Mutation characteristics of extreme precipitation

To further determine the temporal variation features of extreme precipitation, the mutation characteristics were analyzed by utilizing the heuristic segmentation method in the Sichuan province and three subregions. Figure 6 shows the segmentations and change points of the representative index CDD. Three abrupt change points in 1962, 1989, and 2008 were detected by the heuristic segmentation method, where the $P(t_{max})$ and the segment length l_0 are larger than 0.95 and 30, respectively. The change point results of the indices are shown in Table 8. R20, R25, CWD, and SDII did not demonstrate abrupt change points in the Sichuan province. The abrupt change point of SDII was not detected in the Sichuan

province. In the Sichuan province and the three subregions, most of the break points occurred in 1979 and 1991. The Sichuan province and the three subregions experienced notable climate change because abrupt change points were observed for most of the indices. More than five abrupt change points were observed in RX1day for the Sichuan basin, R95 for the southeast Sichuan plateau, PRCPTOT for the Sichuan province and subregions, and PRCPTOT for the Sichuan province and southeast Sichuan plateau.

3.3.2 Periodic characteristics of extreme precipitation

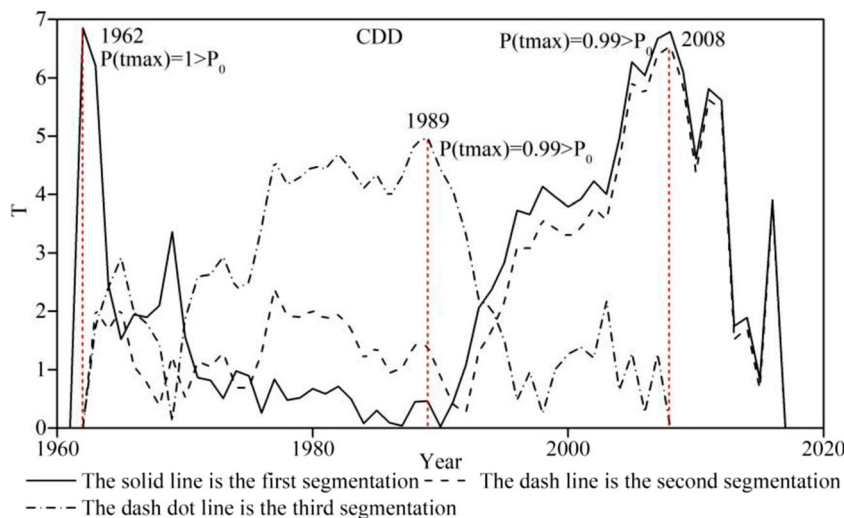
Figure 7 shows the continuous wavelet power spectrum of RX1day, R95, and CWD in the Sichuan province. Multiple cycles are apparent in the extreme precipitation indices. Extreme precipitation is fluctuation processes in the Sichuan province. RX1day and R95 have a 4–8-year period, which passes the 95% confidence level. Figure 7a shows that RX1day has three strongly significant periods with a 1–2-year signal from 1995 to 1998, a 6-year oscillation signal from 1972 to 1976, and a 12-year oscillation signal from 1998 to 2003. Figure 7b shows that R95 has a strongly significant period with a 4–8-year signal from 1969 to 1980, and a slightly significant period with a 1–20-year signal from 1993 to 1998. Figure 7c shows that CWD has a strongly significant period with a 4-year oscillation signal from 1991 to 1995, and a 3–5-year signal from 2007 to 2010.

Table 7 Decadal trend rates (mm/10a) of precipitation indices in three subregions

Season	Index	Sichuan basin		Northwest Sichuan plateau		Southwest Sichuan plateau	
		Average value	Trend	Average value	Trend	Average value	Trend
Spring	RX1day	73.37	0.38	30.67	<i>1.19</i>	42.86	1.48
	RX5day	114.93	-1.03	57.94	<i>2.80</i>	76.53	3.67
Summer	RX1day	193.68	1.41	71.17	0.89	130.29	2.17
	RX5day	314.56	4.06	155.97	1.48	244.47	0.28
Autumn	RX1day	87.47	-1.79	44.31	0.31	62.77	-0.14
	RX5day	160.77	-3.93	89.77	0.10	121.43	-0.73
Winter	RX1day	16.10	0.17	5.51	0.26	9.65	-0.40
	RX5day	28.05	0.05	11.84	0.30	14.91	-0.40

Italic values indicate that the index trend is statistically significant

Fig. 6 Representative segmentations and change points of CDD indices



Relationships between indices of extreme precipitation and indices of the ocean-atmospheric climate from 1961 to 2017

The ocean-atmospheric circulation of SASMI, EASM, and ENSO events exhibit strong correlations with the indices of extreme precipitation in the Sichuan province. The ENSO events have the longest and strongest relations with extreme precipitation in the Sichuan province. The extreme precipitation indices are influenced more by EASM than SASMI in this region. Moreover, both SASMI and EASM have a statistically positive correlation with R95 from 1994 to 1995 and with CWD from 1990 to 1995.

3.4 Connection between SASMI/EASM and extreme precipitation indices

The Sichuan province is a typical monsoon climate region influenced by the SASM and EASM. In Figs. 8 and 9, we

depict the relationships between the SASM/EASM and RX1day/R95/CWD by using the CWT. Here, the duration, intensity, and frequency of extreme precipitation are represented by RX1day, R95, and CWD, respectively.

The spectrum of CWT between SASM and extreme precipitation indices is shown in Fig. 8. Figure 8a shows that RX1day has a 1–2-year signal of negative correlation from 1995 to 1997 and a 1–2-year signal of statistically significant positive correlation with SASM from 1972 to 1977. Figure 8b shows that R95 has a 1–2-year signal of positive correlation and a 4–5-year signal of statistically significant negative correlation with SASM from 1990 to 1995, and a 1–2-year signal and a 7-year oscillation signal from 1970 to 1972. Figure 8c shows that CWD displays a statistically significant negative correlation with SASM with a 3–5-year signal from 1990 to 1994 and a 1.5-year oscillation signal from 1976 to 1978. These results

Table 8 Abrupt change points in the Sichuan province and three subregions

Extreme precipitation index	Sichuan province	Sichuan basin	Northeast Sichuan plateau	Southeast Sichuan plateau
R10 (d)	2013	1968, 1990	1974, 1975, 2001	1964, 1969, 2004, 2014
R20 (d)	–	1986, 1988	–	1964
R25 (d)	–	–	–	1983
CDD (d)	1962, 1989, 2008	1986, 1989	1962, 1989, 2008	1981, 2008
CWD (d)	–	1966	1974, 1975, 2011	2012
RX1day (mm)	1978, 2009, 2004, 2015	1988, 1991, 1944, 1996, 1997, 2004, 2015	1979	1983
RX5day (mm)	1979, 1991, 2009	1985, 2008	1970, 2005, 2010	1969, 1989
R95 (mm)	1979, 1991, 2011,	1991, 2010, 2014	1979, 2011	1964, 1969, 1997, 2003, 2013
R99 (mm)	1979, 1985, 2009	1991, 2009, 2015	1965, 1992	1983, 2011
PRCPTOT (mm)	1979, 1993, 1997, 2005, 2011	1990	1974, 2005, 2011	1964, 1969, 1983, 2008, 2013
SDII (mm/d)	–	–	–	–

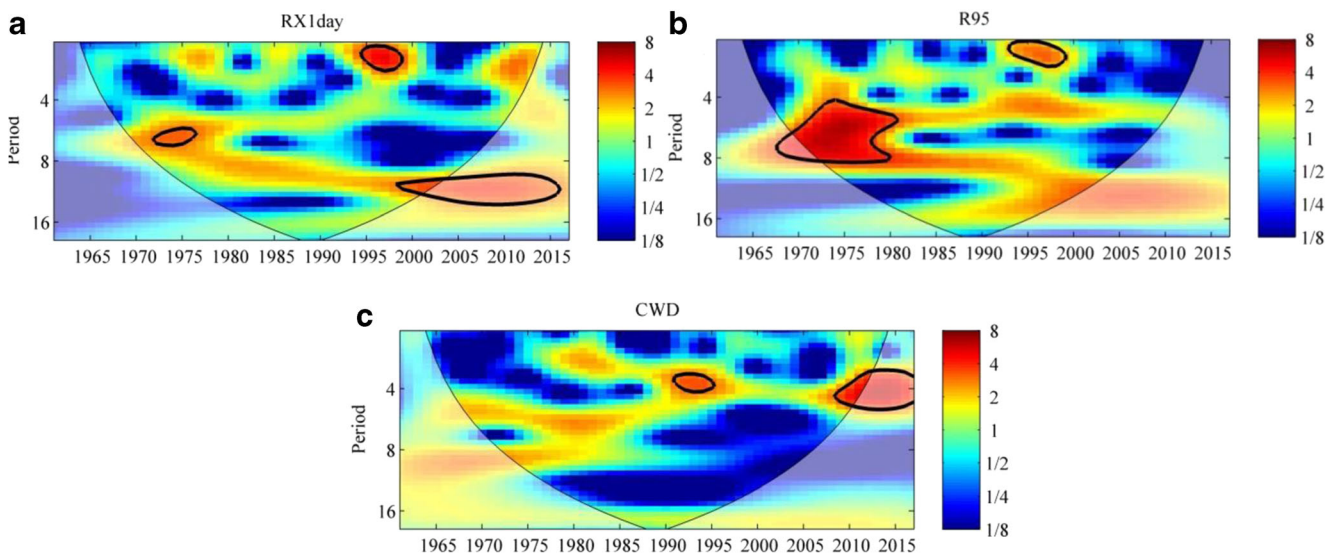


Fig. 7 The CWT power spectrum of **a** RX1day, **b** R95, and **c** CWD in the Sichuan province. Significant relations are denoted by the thick black contour, which is at the 5% level. The lighter shades indicate the cone

of influence, which is explained in previous work (Grinsted et al. 2004). Wavelet energy is expressed by the color bar on the right

indicate that the variations in the duration, intensity, and frequency of extreme precipitation are significantly associated with the SASM, irrespective of the extent of positive or negative correlations in the Sichuan province.

Figure 9 displays the spectrum of cross-wavelet transforms between the EASM and extreme precipitation indices. Three statistically significant positive correlations between the EASM and RX1day are depicted in Fig. 9a, which are an obvious 1–3-year signal from 1993 to 2000 and 2008–2010, and an 8–10-year signal from 1980 to 1987. Figure 9b shows five statistically significant positive correlations between the EASM and RX1day, which include an obvious 1–2-year signal from 1994 to 2000, a 2–3-year signal from 1980 to 1983, a 4–5-year signal from 1986 to 1990, a 5–6-year signal from 1970 to 1977, and a long 8–11-year signal from 1981 to 1988. Figure 9c shows that the EASM has a 1–4-year signal of statistically significant positive correlation with the EASM from 1978 to 2000. These statistically significant positive correlations indicate that the EASM in the Sichuan province is significantly associated with changes in the duration, intensity, and frequency of extreme precipitation.

According to the distribution of wavelet energy shown in Figs. 8 and 9, the influence of the EASM on extreme precipitation is stronger than that of the SASMI. This demonstrates that the extreme precipitation is influenced more by the EASM than the SASMI in the Sichuan province. Moreover, both SASMI and EASM have a statistically positive correlation with R95 from 1994 to 1995 and with CWD from 1990 to 1995.

3.5 Connection between indices of extreme precipitation and ENSO events

As precipitation decreases during warm phase periods of El Niño events and increases during cool phase periods of La Niña events in the Sichuan province (Ouyang et al. 2014), we reveal that ENSO events have the longest and strongest correlations with the duration, intensity, and frequency of extreme precipitation compared with the SASM and EASM. Figure 10a shows that ENSO events display statistically significant negative correlations with RX1day with a 2-year oscillation signal from 1996 to 1998, a 5–6-year signal from 1988 to 1991, a strong 10–13-year signal from 1995 to 2003, and a positive correlation with a 2-year oscillation signal from 2008 to 2010. Figure 10b shows that ENSO events display a statistically significant positive correlation with R90, with a long and strong 2–7-year signal from 1970 to 2000. Moreover, the 2–7-year signal changes to a 5–6-year signal in the boundary year of 1976. Figure 10b shows that ENSO events display statistically significant negative correlations with R90, with a 3–4-year signal from 1984 to 1986, a 1–2-year signal from 1995 to 1996, and a strong 12-year oscillation signal from 1998 to 2001. Figure 10c shows that ENSO events display statistically significant positive correlations with CWD, with a long 2–5-year signal from 1980 to 2000 and a 5–6-year signal from 1988 to 1991. Compared with the cross-wavelet spectra for the SASMI and EASM, the ENSO events have the longest and strongest association with the duration, intensity, and frequency of extreme precipitation in the Sichuan province.

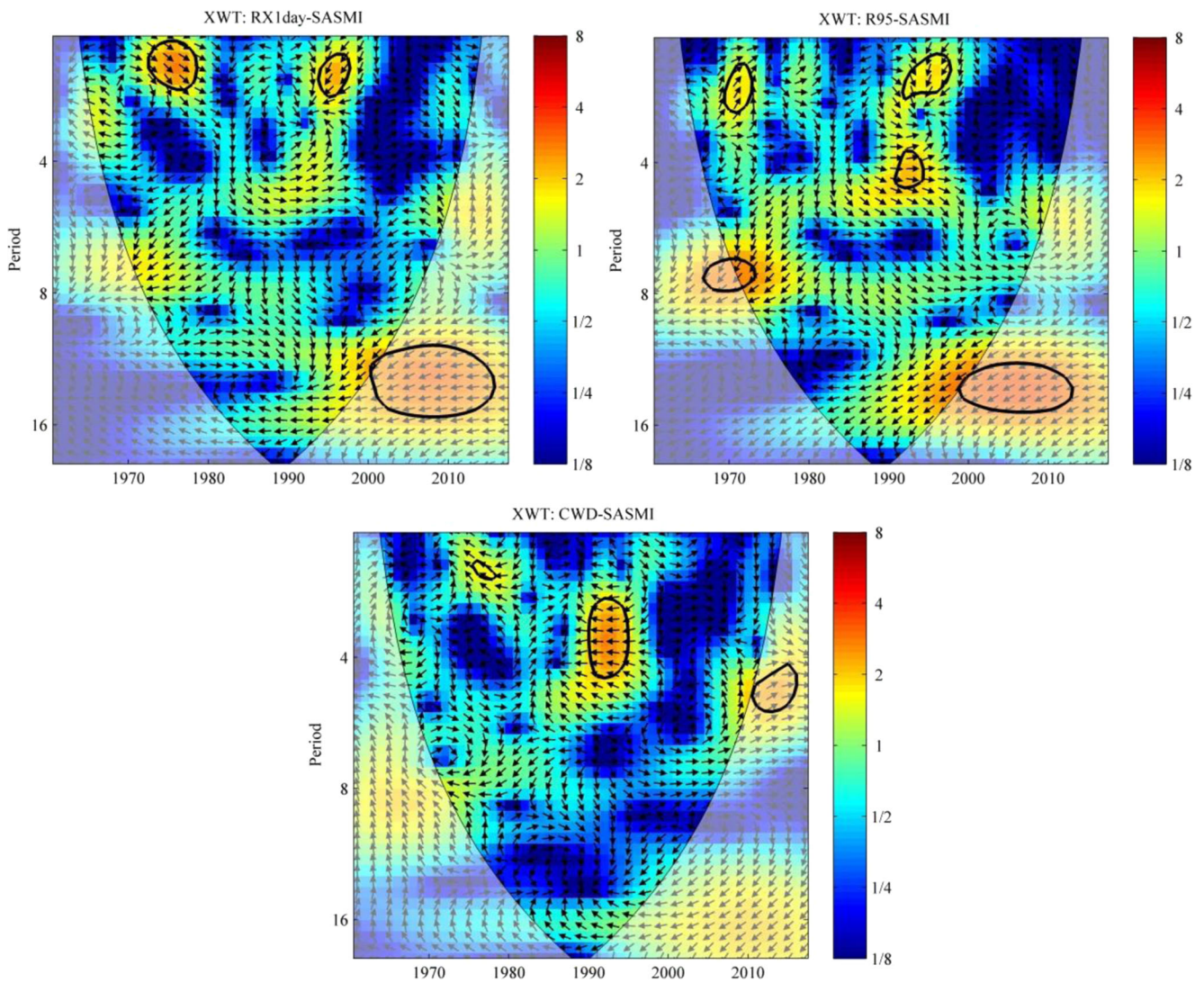


Fig. 8 The CWT spectrum of the SASMI and representative indices of extreme precipitation (RX1day, R95, and CWD) in the Sichuan province. Significant relations are denoted by a thick black contour, which is at the 5% level of significance. The lighter shades indicate the cone of influence, which is explained in the previous work (Grinsted 2004).

The relationship of the relative phase can be justified by the right-hand screw rule. The thumb pointing to the outside/inside of the paper indicates the positive/negative relationship. Wavelet energy is expressed by the color bar on the right

4 Discussion

The discussion will cover the two aspects of this research.

- (1) The regional differences in extreme precipitation indices were influenced by the complex local geography, dramatically increased human activity, and source transportation of water vapor.

Table 9 shows the changes in 11 extreme precipitation indices in the Sichuan province, the central Himalayas, southwestern China, and the Hengduan mountains. Comparison of the trends of each region showed that there are regional differences in the higher and lower

altitudes. In our case, the northwest Sichuan plateau and the southwest Sichuan plateau (higher altitudes) exhibited increasing trends. However, the Sichuan basin (lower altitude) exhibited decreasing trends. Therefore, it is reasonable to conclude that regional differences exist in higher altitudes and lower altitudes in Sichuan. These results may be affected by the special geographical position and complex local geography and monsoons, corresponding with previous studies (Zhang and Ma 2011; Yuan et al. 2014; Zhou and Lei 2018). The eastern part of Sichuan is a basin with an average elevation of 500 m, whereas the average elevation exceeds 3000 m in the northwest Sichuan plateau and southwest Sichuan plateau. The geographic elevation variation is the direct

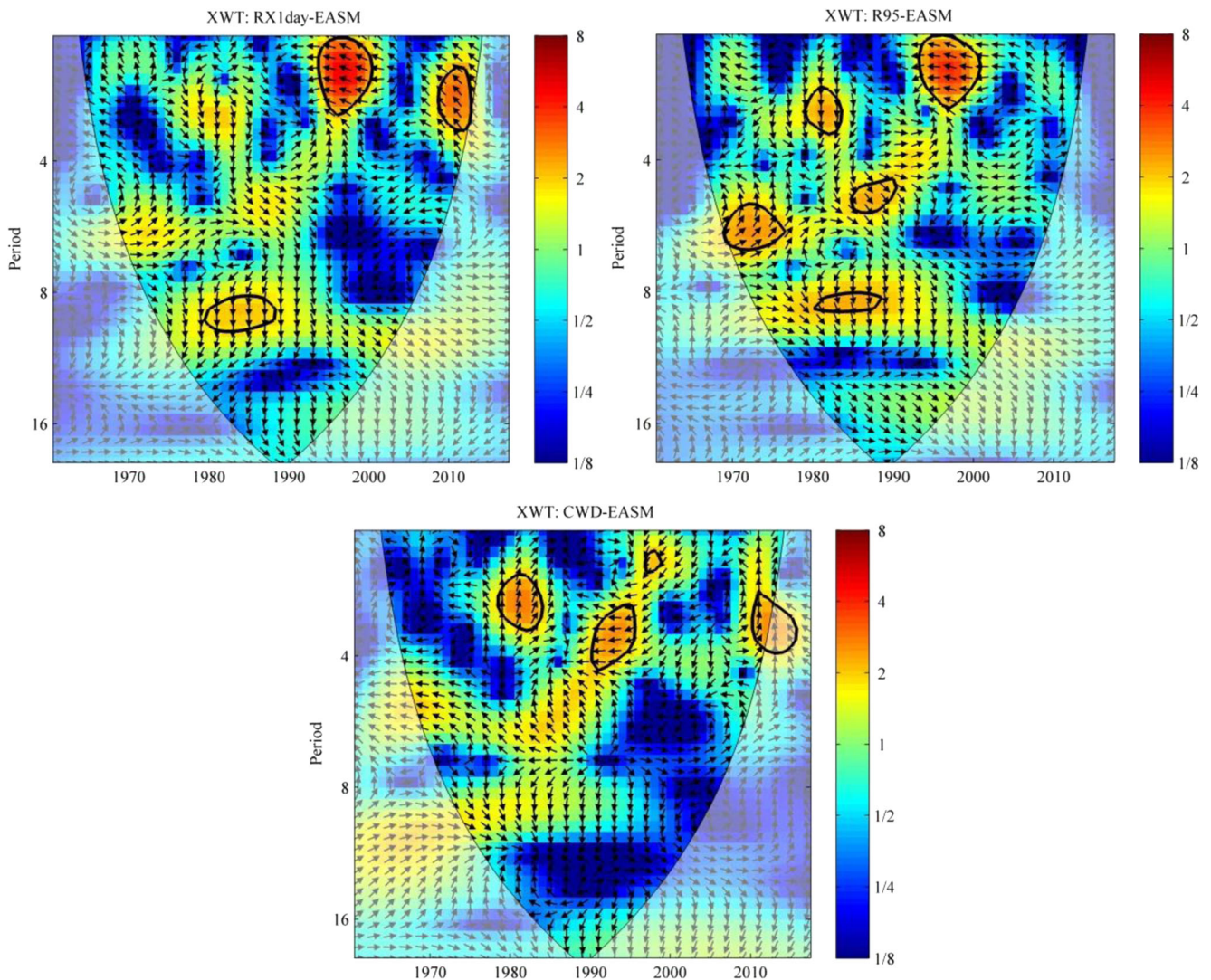


Fig. 9 The CWT spectrum of the EASM and representative indices of extreme precipitation (RX1 day, R95, and CWD) in the Sichuan province

cause of extreme precipitation changes (Liu and Xu 2016; Krishnan et al. 2018). Moreover, the Sichuan province has a population of 83.02 million RMB and a total GDP of 3698.02 billion RMB according to the 2017 statistical bulletin for Sichuan's national economic and social development. The population and economy differ greatly between the western Sichuan province and the Sichuan basin. Therefore, those regions suffer from more serious soil erosion, landslides, floods, and droughts to varying extents. In addition, the source transportation of water vapor is different in western Sichuan and the Sichuan basin. Western Sichuan is more influenced by the SASMI, whereas the Sichuan basin is more influenced by the EASM (Li et al. 2009; Zhou and Lei 2018). Overall, the regional differences in extreme precipitation indices are influenced by the complex local geography, dramatically increased human activity, and source transportation of water vapor (Tandon et al. 2018).

- (2) Extreme precipitation indices will slightly increase and decrease in the Sichuan plateau and Sichuan basin, respectively. However, extreme precipitation events in the future will increase sharply under the influence of the ocean-atmospheric climate, such as ENSO events.

According to the China Meteorological Administration, the average precipitation is 521.7 mm from May to July in the Sichuan province, which is higher than the average precipitation of 421 mm from May to July 1961–2017. The daily precipitation at the Pengzhou and Qingchuan stations were 232.9 and 225 mm, respectively, on July 10, 2018, which is higher than the records of each station. Extreme precipitation events during May–July 2018 caused the loss of 3 billion RMB. However, our result and a related reference (Zhou and Lei 2018) show

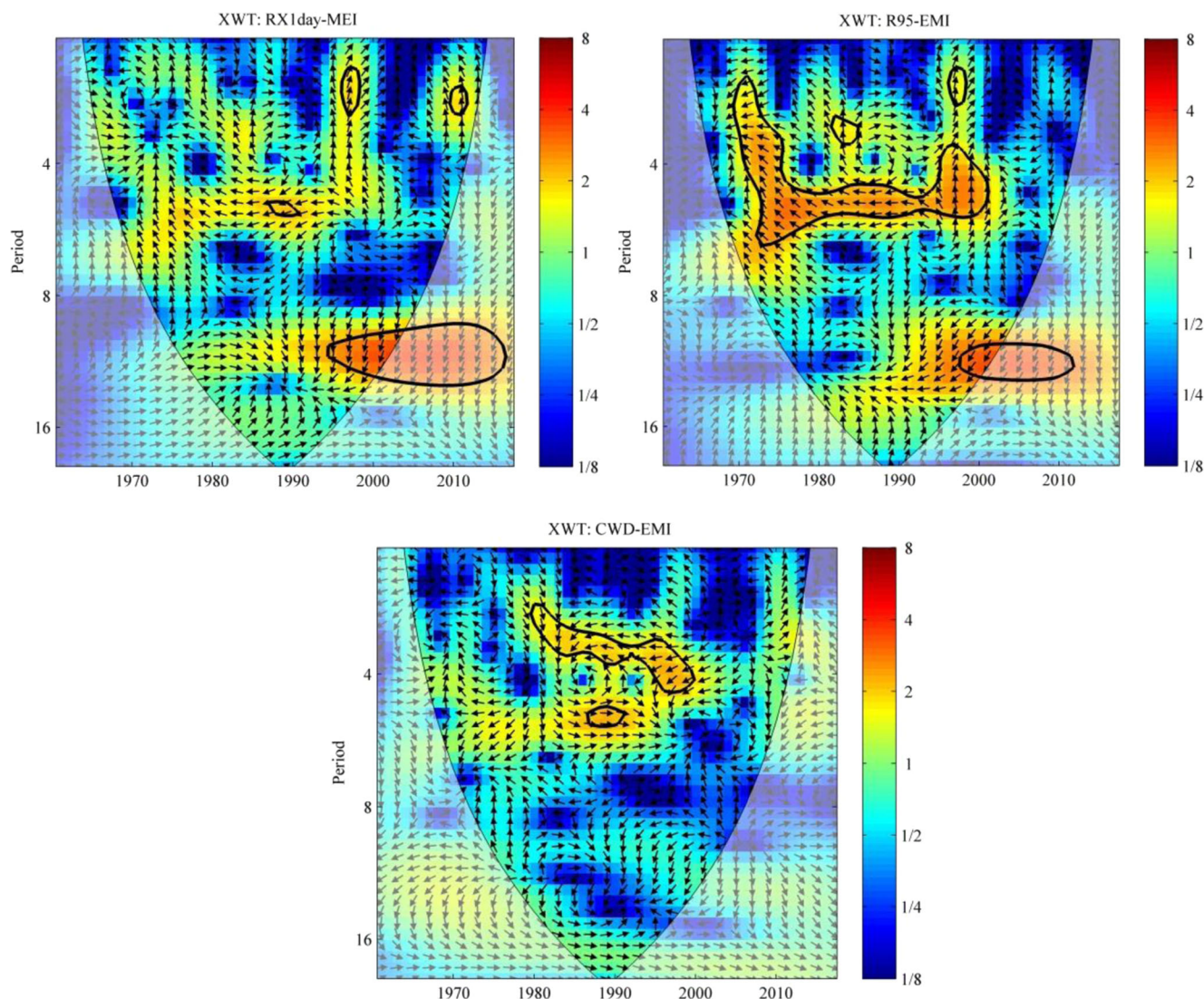


Fig. 10 The CWT spectrum of ENSO events and representative indices of extreme precipitation (RX1day, R95, and CWD) in the Sichuan province

the intensity and frequency of extreme precipitation will decrease but their duration will not change in the Sichuan basin. This indicates that the ocean-atmospheric climate clearly influenced extreme precipitation in the Sichuan province in 2018. From the indices of extreme precipitation and climate circulation, ENSO events have the strongest and longest correlation with extreme precipitation. Furthermore, 2018 is a year in which La Niña occurs (Shi et al. 2018b). Therefore, it is reasonable to conclude that ENSO events were the dominant factor influencing May–July 2018 extreme precipitation in the Sichuan basin. This result indicates that the extreme precipitation events in some years will increase dramatically under the influence of the ocean-atmospheric climate, such as ENSO events. Although the 2018 extreme precipitation occurred in the Sichuan province, the spatiotemporal variations of extreme precipitation indices will not fundamentally change.

5 Conclusions

In this research, the spatiotemporal variations in extreme precipitation indices were determined in the Sichuan province. In general, the values of regional trends constitute slight changes from -0.02 – 2.91 . This indicates that the changes in extreme precipitation should be minor in the future. The Sichuan province and the three subregions experienced notable climate change indicated by the mutation technique because abrupt change points were observed for most indices. Additionally, the change in extreme precipitation is a fluctuating process. Spatially, there may be contrary trends in extreme precipitation indices in the higher altitude and lower altitude regions of the Sichuan province. The northwest and southwest Sichuan plateau (higher altitudes) showed increasing trends. However, the Sichuan basin (lower altitudes) exhibited decreasing trends. Our results also show that the

Table 9 Decadal trends in extreme precipitation in the Sichuan province and other natural transition regions at higher altitudes and lower altitudes

Indices	Northwest Sichuan plateau (1961–2017)	Southwest Sichuan plateau (1961–2017)	Sichuan basin (1961–2017)	Southern slopes of the central Himalayas (1975–2009)	Northern slopes of the central Himalayas (1975–2009)	Southwestern China (1961–2008)	Hengduan mountains (1961–2012)
CDD	0.23	0.65	0.65	4.2	0.9	−0.05	−0.56
CWD	0.05	0.06	−0.23	4.7	−0.4	−0.08	0.12
R10	0.53	0.19	−0.44	1.17	−0.07	0	0.15
R20	0.14	0.16	−0.21	0.73	−0.18	0	0.03
R25	0.08	0.25	−0.11	0.6	−0.1	0.02	0.09
RX1day	0.49	0.81	−0.32	−1.7	−1.5	0.05	1.45
RX5day	1.05	−0.18	0.58	3.9	−0.12	0.03	−1.2
R95	4.61	10.63	−2.38	2	−0.9	0.04	4.21
R99	2.24	9.72	0.34	−	−	0.05	1.5
SDII	0.16	0.15	0.06	−0.13	0.04	0.03	0.03
PRCPTOT	13.99	7.73	−15.47	41	−3.7	0.03	5.05
Data source		Our results		(Sigdel and Ma 2016)		(Li et al. 2012b)	(Zhang et al. 2014b)

Italic values indicate that the trend is statistically significant. “−” indicates that the trend was not reported

ocean-atmospheric circulation of SASM, EASM, and ENSO events exhibited good correlations with extreme precipitation in the Sichuan province. This demonstrates that indexes of ocean-atmospheric climate may be utilized to substantially improve the management of extreme water hazards and prediction of extreme precipitation in the Sichuan province.

Acknowledgements The authors gratefully thank the China Meteorological Administration for providing daily precipitation data for the Sichuan province. The authors also thank the Li Jianping research group for providing the SASMI and EASMI data. We are also grateful to Dr. K. Wölter for providing the MEI data. Finally, the authors gratefully thank the anonymous reviewers of this manuscript for the detailed comments.

Funding information This study was supported by Increasing Resilience to Natural Hazards in Earthquake Prone Regions in China: the National Natural Science Foundation of China (Grant Nos. 41661134012 and 416711112) and the talent introduction project of Sichuan University of Science and Engineering (Grant No. 2018RCL09).

Publisher's note Springer Nature remains neutral with regard to jurisdictional claims in published maps and institutional affiliations.

References

- Alexander LV et al (2006) Global observed changes in daily climate extremes of temperature and precipitation. *J Geophys Res Atmos* 111(D5):1042–1063
- Bai YY, Zhang Y, Gao YH, Ze-Neng HE, Yong-Hua LI (2011) Spatial differences of precipitation over Sichuan Basin. *Sci Geogr Sin* 31(4):478–484
- Bernaolagalván P, Ivanov PC, Nunes LA, Stanley HE (2001) Scale invariance in the nonstationarity of human heart rate. *Phys Rev Lett* 87(16):168105–1–168105–4
- Bezerra BG, Silva LL, Silva CMSE, Carvalho GGD (2018) Changes of precipitation extremes indices in São Francisco River basin, Brazil from 1947 to 2012. *Theor Appl Climatol* D4:1–12
- Bi B, Zhang X, Dai K (2017) Characteristics of 2016 severe convective weather and extreme rainfalls under the background of super El Niño. *Chin Sci Bull* 62(9):928–937
- Deng Y, Jiang W, He B, Chen Z, Jia K (2018) Change in intensity and frequency of extreme precipitation and its possible teleconnection with large-scale climate index over the China from 1960 to 2015. *J Geophys Res Atmos* 123(4):2068–2081
- Fan X, Xu Q, Scaringi G, Dai L, Li W, Dong X, Zhu X, Pei X, Dai K, Havenith HB (2017) Failure mechanism and kinematics of the deadly June 24th 2017 Xinmo landslide, Maoxian, Sichuan, China. *Landslides* 14(6):2129–2146
- Gao L, Huang J, Chen X, Chen Y, Liu M (2018) Contributions of natural climate changes and human activities to the trend of extreme precipitation. *Atmos Res* 205:60–69
- Gilbert RO (1988) Statistical methods for environmental pollution monitoring. Van Nostrand Reinhold Co, New York
- Grinsted A, Moore JC, Jevrejeva S (2004) Application of the cross wavelet transform and wavelet coherence to geophysical time series. *Nonlinear Process Geophys* 11(5/6):561–566
- Hu H, Mao X, Ling L (2009) Temporal and spatial variations of extreme precipitation events of flood season over Sichuan Basin in last 50 years. *Acta Geograph Sin* 64(3):278–288
- Huang S, Huang Q, Chang J, Zhu Y, Leng G, Xing L (2015) Drought structure based on a nonparametric multivariate standardized drought index across the Yellow River basin, China. *J Hydrol* 530:127–136
- Huang W, Yang Z, He X et al (2018) A possible mechanism for the occurrence of wintertime extreme precipitation events over South China. *Clim Dyn*:1–18
- Iwona P, Adam C, Dariusz G, Zbigniew WK (2018). Observed changes in extreme precipitation in poland: 1991–2015 versus 1961–1990) *Theor Appl Climatol* D5:1–15

- Jaagus J (2006) Climatic changes in Estonia during the second half of the 20th century in relationship with changes in large-scale atmospheric circulation. *Theor Appl Climatol* 83(1–4):77–88
- Jevrejeva S, Moore JC, Grinsted A (2003) Influence of the Arctic oscillation and El Niño-southern oscillation (ENSO) on ice conditions in the Baltic Sea: the wavelet approach. *J Geophys Res Atmos* 108(D21):4677
- Karl TR, Nicholls N, Ghazi A (1999) Clivar/GCOS/WMO workshop on indices and indicators for climate extremes workshop summary. *Clim Chang* 42(1):3–7
- Kenawy AE, Lópezmoreno JI, Vicenteserrano SM (2011) Recent trends in daily temperature extremes over northeastern Spain (1960–2006). *Nat Hazards Earth Syst Sci* 11(9):2583–2603
- Kong F et al (2017) Advances and prospects of spatiotemporal pattern variation of extreme precipitation and its affecting factors under the background of global climate change. *J Catastrophol* 32(2):165–174
- Krishnan MVN, Prasanna MV, Vijith H (2018) Statistical analysis of trends in monthly precipitation at the limbang river basin, Sarawak (nw borneo), Malaysia. *Meteorog Atmos Phys*. <https://doi.org/10.1007/s00703-018-0611-8>
- Li J, Wu Z, Jiang Z, He J (2009) Can global warming strengthen the east Asian summer monsoon? *J Clim* 23(24):6696–6705
- Li Z et al (2012a) Changes of daily climate extremes in southwestern China during 1961–2008. *Glob Planet Chang* 80–81:255–272
- Li Z et al (2012b) Changes of daily climate extremes in southwestern China during 1961–2008. *Glob Planet Chang* 80(80–81):255–272
- Li X, Wang X, Babovic V (2018) Analysis of variability and trends of precipitation extremes in Singapore during 1980–2013. *Int J Climatol* 38(2):125–141
- Liu L, Xu ZX (2016) Regionalization of precipitation and the spatiotemporal distribution of extreme precipitation in southwestern China. *Nat Hazards* 80(2):1195–1211
- Ma ZF, Liu J, Zhang SQ, Chen WX, Yang SQ (2013) Observed climate changes in Southwest China during 1961–2010. *Adv Clim Chang Res* 4(1):30–40
- Ouyang R, Liu W, Fu G, Liu C, Hu L, Wang H (2014) Linkages between enso/pdo signals and precipitation, streamflow in China during the last 100 years. *Hydrol Earth Syst Sci* 18(9, 11(4)):3651–3661
- Salmi T, Määttä A, Anttila P, Ruoho-Airola T, Amnell T (2002) Detecting trends of annual values of atmospheric pollutants by the Mann-Kendall test and Sen's slope estimates—the excel template application MAKESENS. Finnish Meteorological Institut, Report code FMI-AQ-31, Helsinki, pp 35
- Sedmeier K, Feldmann H, Schädler G (2018) Compound summer temperature and precipitation extremes over Central Europe. *Theor Appl Climatol* 131(3–4):1493–1501
- She D, Xia J, Song J, du H, Chen J, Wan L (2013) Spatio-temporal variation and statistical characteristic of extreme dry spell in Yellow River Basin, China [J]. *Theor Appl Climatol* 112(1–2):201–213
- Shi J, Cui L, Wen K, Tian Z, Wei P, Zhang B (2018a) Trends in the consecutive days of temperature and precipitation extremes in China during 1961–2015. *Environ Res* 161:381–391
- Shi YF, Yang YZ, Wu KJ, Sun BN (2018b) The signal of La Niña in wave transport. *Int J Appl Earth Obs Geoinf* 70:118–124
- Sigdel M, Ma Y (2016) Variability and trends in daily precipitation extremes on the northern and southern slopes of the central Himalaya. *Theor Appl Climatol* 130(1–2):571–581
- Sigdel M, Ma Y (2017) Variability and trends in daily precipitation extremes on the northern and southern slopes of the central Himalaya. *Theor Appl Climatol* 130:1–11
- Sun J, Zhang F (2017) Daily extreme precipitation and trends over China. *Sci China Earth Sci* 60(12):2190–2203
- Sun W, Mu X, Song X, Wu D, Cheng A, Qiu B (2016) Changes in extreme temperature and precipitation events in the loess plateau (China) during 1960–2013 under global warming. *Atmos Res* 168(22):33–48
- Tandon NF, Zhang X, Sobel AH (2018) Understanding the dynamics of future changes in extreme precipitation intensity. *Geophys Res Lett* 45:2870–2878. <https://doi.org/10.1002/2017GL076361>
- Wang XL (2008a) Accounting for autocorrelation in detecting mean-shifts in climate data series using the penalized maximal t or F test. *J Appl Meteorol Climatol* 47:2423–2444
- Wang XL (2008b) Penalized maximal F-test for detecting undocumented mean-shifts without trend-change. *J Atmos Ocean Technol* 25(3):368–384
- Wang S, Zhang M, Wang B, Sun M, Li X (2013) Recent changes in daily extremes of temperature and precipitation over the western Tibetan plateau, 1973–2011. *Quat Int* 313–314(6):110–117
- Wolter K, Timlin MS (2011) El Niño/southern oscillation behaviour since 1871 as diagnosed in an extended multivariate ENSO index (MEI.Ext). *Int J Climatol* 31(14):1074–1087
- Xu C, Luo Y, Xu Y (2011) Projected changes of precipitation extremes in river basins over China. *Quat Int* 244(2):149–158
- Yin YP, Wang WP, Zhang N, Yan JK, Wei YJ (2017) The June 2017 Maoxian landslide: geological disaster in an earthquake area after the Wenchuan Ms 8.0 earthquake. *SCIENCE CHINA Technol Sci* 60(11):1–5
- Yuan WD, Zheng JK, Dong K (2014) Spatial and temporal variation in extreme precipitation events in southwestern China during 1962–2012. *Resour Sci* 36(4):0766–0772
- Zhang S, Ma Z (2011) Change tendency and cyclicity analysis of extreme precipitation over Sichuan Province during 1961–2009. *J Nat Resour* 26(11):1918–1929
- Zhang Q, Peng J, Singh VP, Li J, Chen YD (2014a) Spatio-temporal variations of precipitation in arid and semiarid regions of China: the Yellow River basin as a case study [J]. *Glob Planet Chang* 114(2):38–49
- Zhang K, Pan S, Cao L, Wang Y, Zhao Y, Zhang W (2014b) Spatial distribution and temporal trends in precipitation extremes over the Hengduan Mountains region, China, from 1961 to 2012. *Quat Int* 349:346–356
- Zhang J, Shen X, Wang B (2015) Changes in precipitation extremes in southeastern Tibet, China. *Quat Int* 380–381:49–59
- Zhang Q, Gu XH, Li JF, Shi PJ, Singh VP (2018) The impact of tropical cyclones on extreme precipitation over coastal and inland areas of China and its association to ENSO. *J Clim* 31(5):1865–1880
- Zhao Y, Xu X, Huang W et al (2018) Trends in observed mean and extreme precipitation within the yellow river basin, China. *Theor Appl Climatol* 5:1–10
- Zhou XY, Lei WJ (2018) Complex patterns of precipitation and extreme events during 1951–2011 in Sichuan Basin, southwestern China. *J Mt Sci* 15(2):340–356